Separation of magnesite and calcite based on flotation solution chemistry

Jin Yao, Xiufeng Gong, Haoran Sun, Ruofan He, Wanzhong Yin

School of Resources & Civil Engineering, Northeastern University, Shenyang 110819, Liaoning, China

Corresponding author: G15524147233@163.com (Xiufeng Gong)

Abstract: The dissolution characteristics of minerals, dissolution of flotation agents in solutions, and equilibrium of dissociations and associations serve as the basis for determining the optimal conditions for the effective components of flotation agents and for evaluating the interaction between flotation agents and minerals. This basis provided the theoretical support for the flotation separation of minerals. Based on this, the flotation separation of magnesite and calcite was realized using sodium dihydrogen phosphate, also known as monosodium phosphate (MSP), as a regulator and dodecylamine (DDA) as a collector. When MSP was used in the DDA system, single-mineral and binary mixed-ore flotation tests revealed that the floatability of calcite was significantly greater than that of magnesite and the separation of magnesite and calcite was more effective, respectively. Zeta potential measurements showed that MSP-containing negative groups could selectively reduce the zeta potential of calcite and promote the adsorption of DDA-containing positive groups on the surface of the calcite. However, this effect was negligible on the zeta potential of magnesite. Due to the stronger affinity of MSP to Ca^{2+} than that to Mg^{2+}, as demonstrated by Fourier transform infrared and X-ray photoelectron spectroscopy analyses, the MSP was adsorbed onto the surface of calcite primarily by hydrogen bonds rather than magnesite, which promoted the stronger adsorption of DDA-containing positive groups on the surface of the calcite. As a result, the differences in the floatability of magnesite and calcite were enlarged by MSP. Thus, MSP can be utilized an effective regulator for the efficient separation of magnesite from calcite via reverse flotation.

Keywords: magnesite, calcite, reverse flotation

1. Introduction

As a nonferrous mineral resource, magnesite is widely used mainly as a metallurgical refractory material and is also applied industrially as a sintering solvent, building material, and magnesium metal refining agent (Hou et al., 2021; Yuan et al., 2022). Moreover, due to the current severe phosphorus pollution and resource shortages, magnesite is being used as a magnesium and hydroxyl reagent for recovering phosphorus from urban wastewater (Song et al., 2006). Magnesite is a mineral originates from sedimentary rocks containing organic components. The lack of oxygen, water, and dissolved magnesite in such an environment results in the formation of magnesite mainly in layered or nodular habits (Wei et al., 2019). The nodules are formed by the accumulation of magnesite crystals around a core that grow concentrically and extend to the outer layer (Zhao et al., 2015). The core is generally composed of other minerals such as carbonate minerals represented by calcite (Sanchez-Espana et al., 2002).

The flotation separation of magnesite and calcite, which belong to alkaline earth carbonate minerals, is the most commonly used method in industrial separation (Brik, 2011; Tang et al., 2020; Yang et al., 2020). Furthermore, because magnesite and calcite have similar crystal structures, the active atoms on the main cleavage surface have similar spacing, and calcite has a low hardness(Li et al., 2021). During grinding, calcite usually covers valuable target mineral particles, increasing the difficulty of separation (Tang et al., 2020; Deng et al., 2018). Previous research has demonstrated the considerable solubility of magnesite and calcite in mud, particularly at relatively low pH levels (Luo et

al., 2017). Thus, the ability of obtaining good flotation separation results is based on the use of long-chain collectors with high selectivity (Cases et al., 2002). Furthermore, fatty acids and the C12 alkyl amine are frequently used as collectors in magnesite flotation (Chen and Tao, 2004; Matis, 1988). Currently, the selective separation methods used in case of magnesite and carbonate gangue minerals include direct flotation with anionic collectors (Wang et al., 2016) and reverse flotation with cationic collectors such as amines(Sun et al., 2021). Alternative biotechnology methods for magnesite decalcification with microorganisms were also considered (Yanmis et al., 2015). Sodium oleate is a commonly used anionic collector with strong collection capacity with poor selectivity for many minerals, including magnesite (Sun et al., 2020). Other traditionally used fatty acid type collectors have similar limited selectivity (Gao et al., 2015; Momenzadeh et al.). Tang et al. analyzed the surface chemistry of magnesite and calcite in a potassium cetyl phosphate flotation system and observed strong displacement of the zeta potential of the adsorbed magnesite in the negative direction (Tanget al., 2020). They concluded that the magnesite adsorption process was spontaneous and collector adsorption involved a chemical adsorption process at magnesite surface, thus direct flotation of magnesite could be occurred. A.E.C. Botero et al. studied the affinity of *Rhodococcus opacus* as a flotation collector on the calcite and magnesite surfaces; they concluded that magnesite had better interaction with this species (Botero et al., 2008; Casas Botero et al., 2007). The most recent research in this field focuses on magnesite separation via reverse flotation with cationic collectors such as amines (Yang et al., 2020; Wonyen et al., 2018; Yao et al., 2016; Teng et al., 2018).

In our previous study (Yao et al., 2021), it was observed that sodium dihydrogen phosphate can effectively improve the separation effect of magnesite and dolomite through reverse flotation test and density functional theory analysis in the system with DDA as a collector. Based on this, the mechanism of reagent action for separating magnesite and calcite was investigated from the perspective of flotation solution chemistry. Furthermore, the influence of the two minerals on the single-mineral and binary mixture floatability was explored through a microflotation experiment to study the different characteristics of magnesite and calcite floatabilities. In addition, zeta potential measurement, Fourier transform infrared (FTIR) analysis, and X-ray photoelectron spectroscopy (XPS) are conducted to evaluate the adsorption behavior of the collectors on these minerals under the action of MSP.

2.   Materials and methods

2.1. Materials and reagents

The single mineral sample of magnesite and calcite used in the test were received from the Dashiqiao area, Liaoning Province, Northeast China. Fig. 1 shows the X-ray diffraction (XRD) patterns of magnesite and calcite samples and Table 1 shows their chemical multielement compositions. The mineral composition was determined via XRD and the single-mineral samples chemical composition analysis. The analysis results showed that the magnesite and calcite used in the test were of high purity, at 95.93% and 99.15%, respectively.
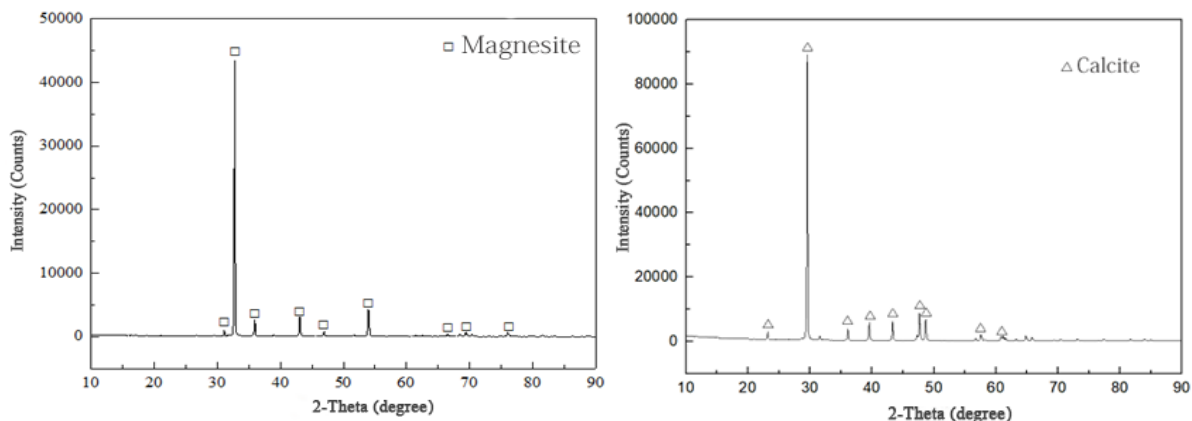
Fig. 1. X-ray powder diffraction patterns of the specimens

Table 1. Chemical compositions of the mineral samples (wt%)

Sample	MgO	CaO	SiO$_2$	Al$_2$O$_3$	Total Fe	Purity
Magnesite	45.68	1.20	0.80	0.055	0.15	95.93
Calcite	0.31	55.55	<0.05	0.22	0.019	99.15

The following preparation methods were applied for the two single mineral samples. An ore block with no impurities on the surface was selected, crushed, and manually screened to keep coarse particles of −0.074–+0.038 mm as test samples. The samples were then processed according to the stacking cone method and sent for chemical component analysis. The analysis results are shown in Table 1. Tianjin Ruijinte Chemical Co. Ltd. provided the MSP used in the test, which was of analytical reagent grade. DDA used in this study was of pure chemical reagent (CP) grade, which was obtained from Sinopharm Chemical Reagent Co. Ltd. Hydrochloric acid and sodium hydroxide were used to adjust the pH value of the solution, and the water used in the test was deionized water.

2.2. Microflotation experiments

An inflatable hanging cell flotation machine (XFG II, Jilin Exploration Machinery Plant, Jilin, China) was used for flotation experiments using single-mineral sample and binary artificial mixed-ore sample (which had a magnesite: calcite ratio of 9:1). The impeller speed of the flotation machine was 1992 rpm. For the flotation experiments, a 2.0 g of each sample was placed in the flotation cell. Then, 20 mL of deionized water was added, and the slurry was mixed for 2 min. Afterward, a pH regulator (hydrochloric acid or sodium hydroxide solution), regulator of MSP (or no regulator), and collector were added in sequence. After stirring for 3 min, the flotation progressed for 3 min. Finally, the foam and sink products were collected, dried, weighed, and analyzed (Yao et al., 2021). The flotation experimental procedure is shown in Fig. 2.
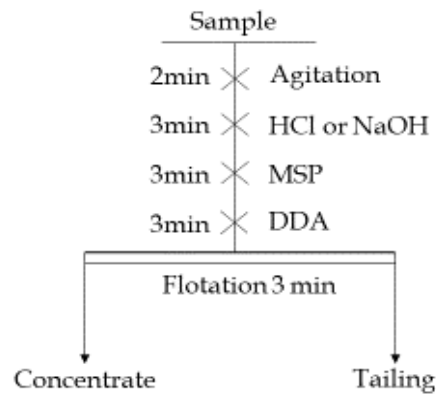
Fig. 2. Flotation tests process

For the single-mineral and binary mixed-mineral flotation experiments, the mineral recovery is calculated using following Eqs. (1) and (2), respectively.

$$\varepsilon = \frac{m_c}{m_c + m_t} \times 100\% \tag{1}$$

In this equation, ε represents the mineral recovery (%), m_t represents the mass of the tailings, and m_c represents the mass of the concentrate.

$$\varepsilon = \frac{\beta m_c}{\beta m_c + \theta m_t} \times 100\% \tag{2}$$

For binary mixed minerals flotation, ε represents the mineral recovery (%), β represents the grade of the concentrate, expressed as CaO or MgO grade (%), and θ represents the grade of the tailings, expressed as CaO or MgO grade (%).

In this study, the recovery results were reported as the average of three independent tests, and the selectivity index (SI) was used to evaluate the separation efficacy of the magnesite–calcite system when the MSP was used. The selectivity index was calculated using Equation (3).

$$SI = \sqrt{\frac{R_m \times J_d}{(100 - R_m) \times (100 - J_d)}} \tag{3}$$

were, SI represents the selectivity index, J_d represents the recovery of calcite in the tailings, and R_m represents the recovery of magnesite in the concentrate.

2.3. Zeta potential measurement

To study the surface electrical properties of the magnesite and calcite particles, the electrokinetic potential was used to determine the zeta potential under different reagent dosages using a Zetasizer Nano ZS90 electrokinetic analyzer (Malvern Instruments Ltd., Malvern, United Kingdom) (Yang et al., 2022). Before each measurement, the mineral samples were ground to less than −5 µm. Then, 20 mg of each sample was weighed and placed into a beaker. Afterward, 40 mL of deionized water was added, and the mixture was stirred with a magnetic stirrer for 2 min to fully disperse the pulp. Hydrochloric acid or sodium hydroxide solutions were added for 3 min to adjust the pulp pH to desired value, and the reagent was added as the same conditions in the flotation experiments. The mixture was stirred for 3 min and then allowed to stand for 20 min. Then, 1 mL of the upper suspension was taken for zeta potential measurements. The average zeta potential value of three easements was reported.

2.4. Fourier transform infrared spectroscopy measurement

To analyze the reagent adsorption at the mineral particle surface, an FTIR spectrometer (Nicolet 460, Thermo Scientific, Waltham, Massachusetts, United States) was used obtain spectra at a resolution of 4 cm^{-1}, within a range of 400–4000 cm^{-1}, and 16 scans. The spectra were analyzed using OMINC™ Spectra™ analysis software (Lu et al., 2011; Yao et al., 2021). For each test, deionized water was added to 2 g of the sample, the slurry was mixed for 2 min, and the pH of the pulp was adjusted with 3 min conditioning time. Then, MSP was added, and the mixture was stirred for 3 min. After vacuum filtration, the solids were washed two or three times with deionized water and were dried at a temperature below 25°C. Afterward, the sample was ground to less than 2 µm. Then, 2 mg of the mineral sample and 200 mg of KBr at a mass ratio of 1:100 were ground, mixed, and pellet was made for FTIR transmission measurement using a tablet presser.

2.5. X-ray photoelectron spectroscopy measurement

For XPS analysis, the mineral samples of magnesite and calcite were scanned separately before and after the conditioning with the reagent using an X-ray photoelectron spectrometer (ESCALAB 25Xi, Thermo Scientific) (Yao et al., 2020). For each test, 2.0 g of the ore sample and the flotation reagent were added according to the required testing conditions. Then, the sample was centrifuged at 3000 rpm for 10 min to separate the solid and liquid components. Then, the obtained solid was washed with deionized water thrice, dried in an oven at a temperature below 25°C, then sample was ready for XPS analysis. When measuring the relative contents of metal ions on the mineral surfaces, the vacuum pressure in the detection process was maintained at 9–10 mbar, and the measurement spectrum was calibrated with the C1s peak of organic carbon; the standard peak was 248.80 eV (Yin et al., 2019). The avantage spectral analysis software was used to fit the obtained scanning map, and the relative atomic contents of carbon, oxygen, magnesium, calcium and other elements on the surfaces of the ore sample were analyzed.

3.   Results and discussion

3.1. Microflotation tests

Under the condition of no regulator and natural pH, the effect of DDA dosage on the floatability of a single mineral was investigated by flotation. The results from flotation experiments are shown in Fig. 3.
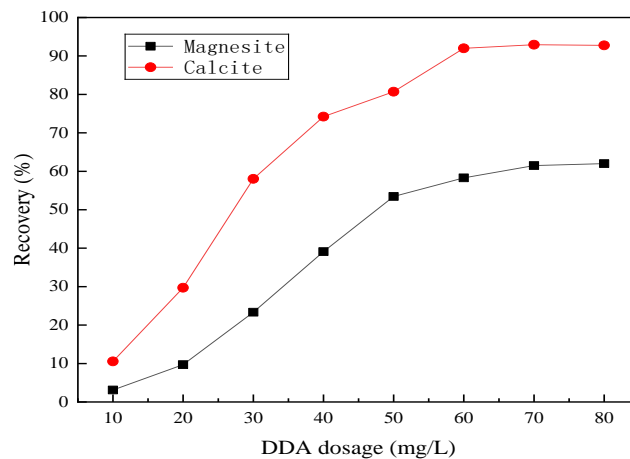
Fig. 3. Effect of DDA dosage on the floatability of magnesite and calcite at pH of 8.9 and 9.5

As shown in Fig. 3, the recovery of magnesite and calcite gradually increased with increasing DDA dosage. When the concentration of DDA increase to 70 mg/L from 10 mg/L, the magnesite recovery increased from 3.10% to 61.50%. Then the recovery percentage tended to remain stable as the concentration of DDA in the solution further increased. The recovery of calcite increased rapidly from 10.55% to 92.00% when the DDA concentration is increased from 10 mg/L to 60 mg/L. Calcite recovery also remained essential as the concentration of DDA increased. Fig. 3 clearly shows the recovery difference of magnesite and calcite at the same DDA dosage. The floatability difference between them was more significant when considering a DDA content of 30 mg/L. At that point, the recovery of magnesite and calcite were 23.35% and 58.05%, respectively. Therefore, a 30 mg/L dosage of DDA was determined to be the prefer collector usage for separation of Calcite from magnesite.

To further investigate the effect of different pulp pH values on the floatability of single minerals. The flotation recover as function of pH for single minerals flotation was evaluated with a fixed DDA dosage of 30 mg/L and the results are shown in Fig. 4.
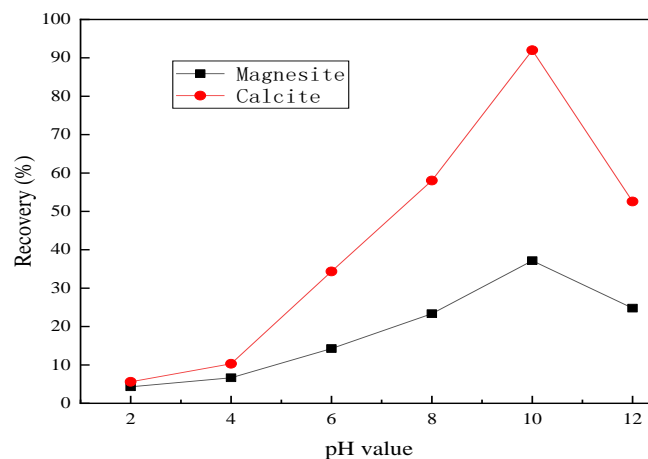
Fig. 4. Effect of pH on the floatability of magnesite and calcite with collector usage of 30 mg/L

As shown in the Fig. 4, the recovery of both minerals first increased and then decreased with an increase in the pulp pH. When the pH increased from ~2 to 10, the magnesite flotation recovery increased from 4.30% to 37.15%. With a further increase in the pulp pH, the magnesite recovery decreased to 24.80%. Under the same condition, calcite recovery significantly increased from 5.35% to 92.00% and then decreased gradually. A comparison of the recoveries of calcite and magnesite at pulp pH values of 8–10 revealed that the greatest difference in the floatability between the two minerals occurred at a pH of ~10, with recoveries of 92.00% for calcite and 37.15% magnesite. Therefore, pH 10 was selected as the best pH pulp value for flotation of calcite. It should point out that even at the

prefer flotation pH and collector usage, about 37.15% of magnesite was still floated. The selective separation can't be achieved.

In order to achieve the effective separation, flotation of mixed two minerals was carried out with MSP regulator. The DDA concentration was set at 30 mg/L, and the pH of the pulp was set at pH 10. The effect of the MSP concentration on the floatability of magnesite and calcite is shown in Fig. 5.
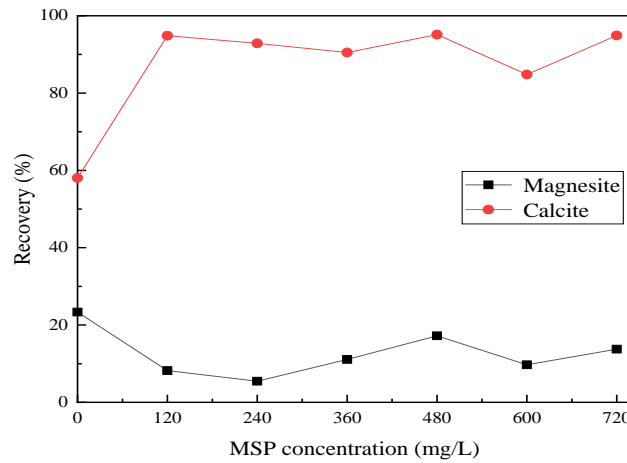
Fig. 5. Effect of MSP dosage on the floatability of magnesite and calcite

As shown in Fig. 5, when the MSP dosage was 0–240 mg/L, the recovery of magnesite decreased from 23.35% to 5.45%, reaching the lowest point. When the MSP dosage was increased subsequently, the magnesite flotation recovery fluctuates around ~15%. The calcite recovery increased rapidly with an increase in the MSP dosage and fluctuated near 92% after reaching the peak value. When the MSP dosage was increased subsequently, the recovery did not change significantly. However, when the MSP was 600 mg/L, the recovery increased from 84.8% to 94.90%. A comparison of the recovery of magnesite and calcite under the different MSP dosages revealed that 240 mg/L of MSP was the best regulator for calcium removal by reverse flotation of magnesite.

Taking MSP and DDA as test conditions with values of 240 and 30 mg/L, respectively, the optimal reverse flotation pH value was studied by changing the pulp pH using MSP as a regulator and DDA as a collector. The experimental results are shown in Fig. 6.
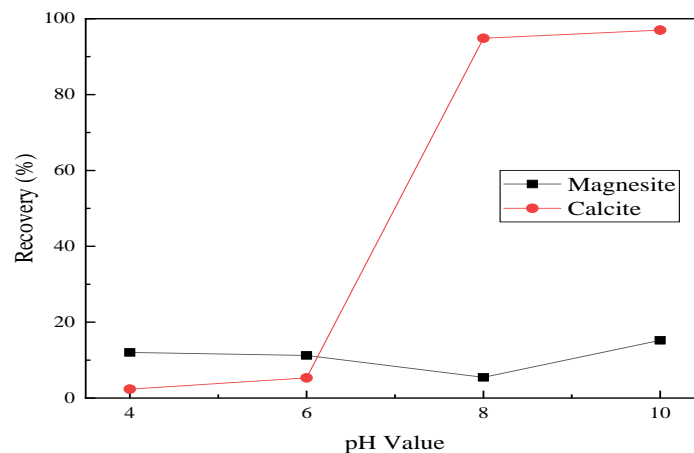
Fig. 6. Effect of pH value on magnesite and calcite floatabilities with NaH_2PO_4

Fig. 6 shows that the magnesite recovery is not sensitive to pH change. The magnesite recovery was stable at 12% with increasing pulp pH. The calcite recovery increased with increasing pH; however, the growth rate differed. When pH increased from 4 to 6, the calcite recovery increases from 2.34% to 5.31%. When pH increased from 6 to 8, the recovery increased sharply from 5.31% to 94.84%, and then the growth rate slowed down. When the pulp pH was ~8–10, the recovery increased from 94.84% to 97.00%. By comparing the recovery of the two minerals when the pulp pH value was 8 and

10, the recovery difference of the two minerals is the largest at pH value of 8. Still, the difference in the two minerals' flotation recovery is not much different under the two pH values. The calcite recovery reaches the maximum when the pulp pH is 10. After careful consideration, the pH of ~10 was selected as the prefer pH condition for separating magnesite and calcite with MSP as a regulator.

To further verify the effect of MSP on the reverse flotation decalcification of magnesite, a flotation test was conducted on a magnesite–calcite binary mixed ore. The specific test data are listed in Table 2.

Table 2. Results of mixed-mineral reverse flotation test

Reagents	Product	Yield (%)	Grade (%)		Recovery (wt%)		SI
			MgO	CaO	Magnesite	Calcite	
pH: 10; DDA: 30 mg/L	Concentrate	79.26	44.65	3.69	82.26	52.26	4.23
	Tailings	20.74	36.79	12.90	17.74	47.74	
	Feed	100.00	43.02	5.60	100.00	100.00	
pH: 10; DDA: 30 mg/L MSP: 240 mg/L	Concentrate	86.43	45.26	2.98	90.93	45.92	11.81
	Tailings	13.57	28.75	22.33	9.07	54.08	
	Feed	100.00	43.02	5.60	100.00	100.00	

When no regulator was added, the concentrate yield of reverse flotation of magnesite under the DDA system was 79.26%; the recoveries of magnesite and calcite were 82.26% and 52.26%, respectively, and the recovery difference was 30.00%. Compared with the condition without a regulator, when MSP was used as a regulator, the flotation of fine mineral increased to 86.43%, the recovery of magnesite was 90.93%, which increased by 8.67 percentage points, and the recovery of calcite was 45.92%, which decreased by 6.34 percentage points. Moreover, the recovery difference of the two minerals was 45.01%, which was ~1.5 times of the recovery difference of the two minerals without regulator. This indicates that the floatability difference between magnesite and calcite in the absence of a regulator cannot be separated effectively only by DDA collection. Simultaneously, CaO grade in tailings without a regulator was 12.90%, the CaO grade was 22.33% with MSP as a regulator, and the change rate of grade was 73.10%, indicating that calcite had realized effective flotation. Thus, the use of MSP as a regulator can promote the flotation of calcite in a DDA system as well as the effective separation of magnesite from calcite. Table 2 shows that the SI values of the magnesite–calcite system with and without the regulator were 11.81 and 4.23, respectively. Therefore, the addition of a regulator is more conducive to the separation of magnesite and calcite.

3.2. Zeta potential measurement

When a reagent is physically or chemically adsorbed onto a mineral surface, its zeta potential changes, which affects the floatability of the mineral. In this study, the effect of MSP on the surface electrical properties was explored by detecting the changes in the zeta potential of magnesite and calcite before and after MSP addition in the DDA system.

The effect of the regulator dosage on the surface electrical properties of the minerals without DDA was evaluated. The pulp pH was set to ~10, and the zeta potentials of the magnesite and calcite were measured at MSP dosages of 120, 240, 360, 480, 600, and 720 mg/L. The measurement results are shown in Fig. 7.

As shown in the Fig., when DDA was not added, the zeta potential of the magnesite showed negligible change when the MSP dosage increased from 120 to 720 mg/L and remained stable at −4

mV. This indicates that the MSP was not adsorbed onto the surface of the magnesite. Conversely, the zeta potential of the calcite decreased rapidly from −1.52 to −24.3 mV when the dosage of MSP increased from 120 to 240 mg/L. When the MSP dosage increased from 240 to 720 mg/L, the zeta potential of the calcite tended to be stable at ~−24 mV. These results show that MSP selectively reduced the zeta potential of calcite but had no effect on that of magnesite.

Then, the effect of MSP dosage on the mineral surface electrical properties in the DDA system was studied. The pulp pH was set to ~10, and the dosage of DDA was 30 mg/L. The zeta potentials of magnesite and calcite in solution were measured when the dosages of MSP were 120, 240, 360, 480, 600, and 720 mg/L. The measurement results are shown in Fig. 8.
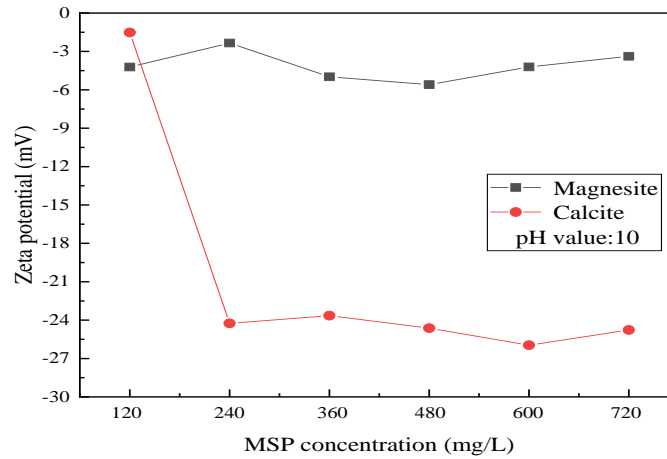
Fig. 7. Effect of regulator dosage on dynamic potential of minerals without DDA
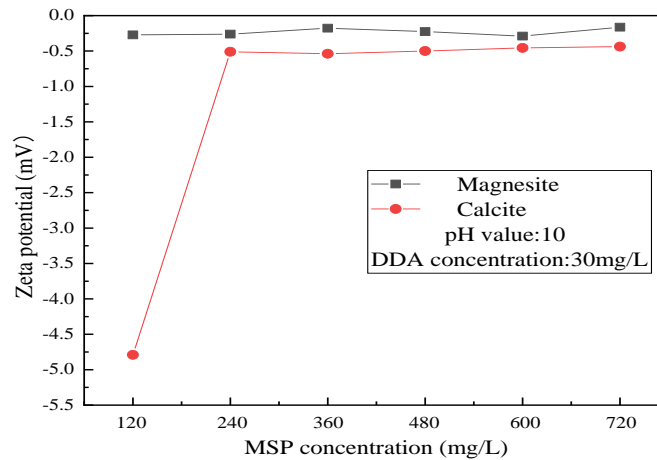
Fig. 8. Effect of MSP dosage on the dynamic potential of minerals in the DDA system

Under the DDA system, the zeta potential of magnesite showed almost no obvious change when the dosage of MSP was increased from 120 to 720 mg/L, and the value remained stable at −0.2 mV. However, the zeta potential of the calcite increased rapidly from −4.79 to −0.511 mV when the dosage of MSP was increased from 120 to 240 mg/L. When the MSP dosage was increased from 240 to 720 mg/L, the zeta potential of the calcite tended to be stable at −0.5 mV.

A comparison of Figs. 7 and 8 reveals that the stable value of the magnesite zeta potential increased from −4 to −0.2 mV, representing an increase of 95%. This indicates that the DDA was adsorbed onto the surface of the magnesite. For calcite, when the dosage of MSP was 120–240 mg/L, the difference in its zeta potential increased with an increase in MSP dosage. When the dosage of MSP was 240 mg/L, the zeta potential difference of calcite was the largest, reaching nearly 23 mV. However, when the dosage of MSP was more than 240 mg/L, the difference in its zeta potential tended to be stable. In summary, MSP-containing negative groups can selectively reduce the zeta

potential of calcite and can promote the adsorption of DDA-containing positive groups on the surface of calcite, although it has little effect on the zeta potential of magnesite.

3.3. Fourier transform infrared measurement

During the infrared spectrum analysis of MSP adsorption at magnesite, the sample was treated in the condition of pH value of ~10 and an MSP dosage of 240 mg/L. The infrared spectrum analysis results before and after the conditioning of the magnesite with the MSP are shown in Fig. 9.
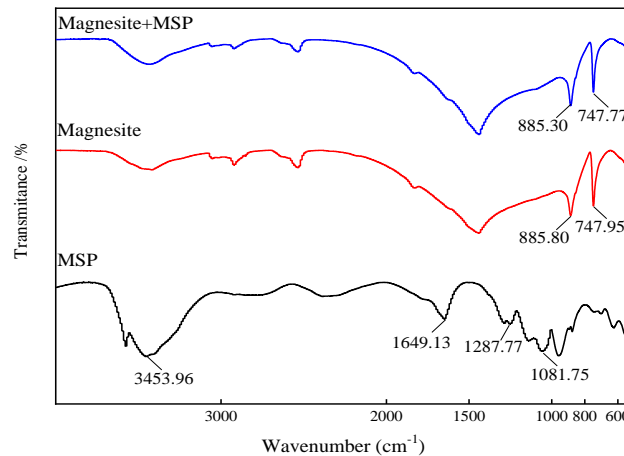
Fig. 9. Fourier transform infrared (FTIR) spectra of magnesite treated with reagents and untreated magnesite

As shown in the Fig., in the infrared spectrum of MSP, the peak at 3453.96 cm^{-1} corresponds to the tensile vibration absorption peak of −OH on MSP and the peak at 1649.13 cm^{-1} corresponds to that of O = P(−OH)$_2$. The peaks at 1287.77 and 1081.75 cm^{-1} correspond to the tensile vibration absorption peaks of P = O and P–O on MSP, respectively (Guo et al., 2017; Shuai et al., 2020). Moreover, magnesite is a carbonate-mineral-containing CO_3^{2-}; 885.80 and 747.95 cm^{-1} are the out of plane bending vibration peak and in-plane bending vibration peak of CO_3^{2-}, respectively (Yao et al., 2020; Sun et al., 2020; Yin et al., 2019). A comparison of the infrared spectra of magnesite before and after the interaction with MSP reveals no significant difference between them, which indicates that the MSP essentially did not adsorb onto the surface of the magnesite.

During the infrared spectrum analysis of calcite, a flotation test was conducted with a pulp pH value of ~10 and an MSP concentration of 240 mg/L. The infrared spectrum analysis results before and after the interaction of the calcite and the reagent are shown in Fig. 10.

Fig. 10 shows that 1431 cm^{-1} is the asymmetric stretching vibration peak of CO_3^{2-} (Yao et al., 2020; Yao et al., 2020). After the interaction between calcite and MSP, the O–H vibration peak appeared peak appeared at 3447 cm^{-1} of calcite, indicating that MSP was adsorbed onto the surface of calcite in
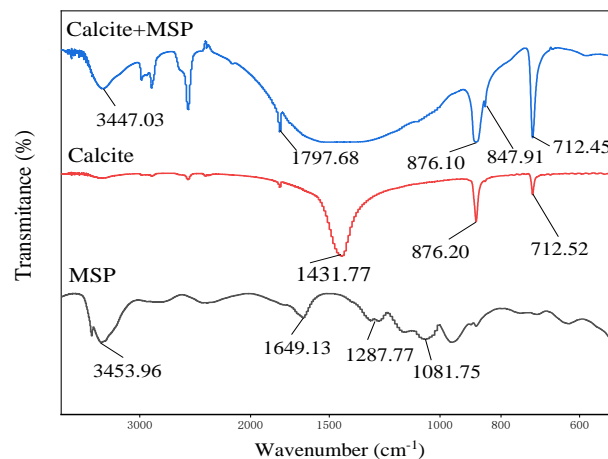
Fig. 10. FTIR spectra of calcite treated with reagents and untreated calcite

the form of hydrogen bonds (Sun et al., 2021). In summary, the MSP was selectively adsorbed onto the calcite surface mainly by hydrogen bonds.

3.4. X-ray photoelectron spectroscopy measurement

Under the conditions of a pulp pH value of 10 and an MSP concentration of 240 mg/L, the reaction mechanism among magnesite, calcite, and MSP was determined and single-mineral XPS measurement was conducted. The results are shown in Table 3.

Table 3. X-ray photoelectron spectroscopy analysis results of samples with and without MSP treatment

Sample	Element % (binding energy, eV)				
	C1s	O1s	Mg1s	Ca2p	P2p
Magnesite	44.40 (284.87)	48.52 (531.38)	7.08 (1304.14)		
Magnesite + MSP	41.34 (284.85)	51.35 (531.60)	7.26 (1304.20)		0.05 (134.29)
Offset	−3.16 (−0.02)	2.83 (0.22)	0.18 (0.06)		0.05 (134.29)
Calcite	40.63 (284.80)	45.64 (531.25)		13.73 (346.84)	
Calcite + MSP	36.68 (284.80)	48.07 (531.30)		14.05 (346.92)	1.20 (133.15)
Offset	−3.95 (0.00)	2.43 (0.05)		0.32 (0.08)	1.20 (133.15)

After adding MSP, the corresponding peak for magnesite appeared at 134.29 eV of the P2p peak; however, the relative element concentration was only 0.05%. On the contrary, when MSP was added for calcite, an obvious corresponding peak appeared at 134.29 eV, and its element relative concentration was 1.20%. This value is 24 times higher than that of magnesite.

Fig. 11 shows that the peak position of Mg1s changed from 1304.14 to 1304.20 eV, and the offset value was 0.06 eV. Moreover, Fig. 12 shows that the peak position of Ca2p changed from 346.84 to 346.92 eV, and the offset value was 0.08 eV. By comparing the two Figs., it can be observed that although the peak of Ca2p changed little compared to Mg1s, the change rate of Mg 1s is 33.33%. This shows that when magnesite and calcite coexist, the MSP reagent will preferentially adsorb onto the calcite surface, which agrees with the flotation test results. The reason for this phenomenon is that the MSP reagent can selectively react with the calcium element rather than the magnesium element.
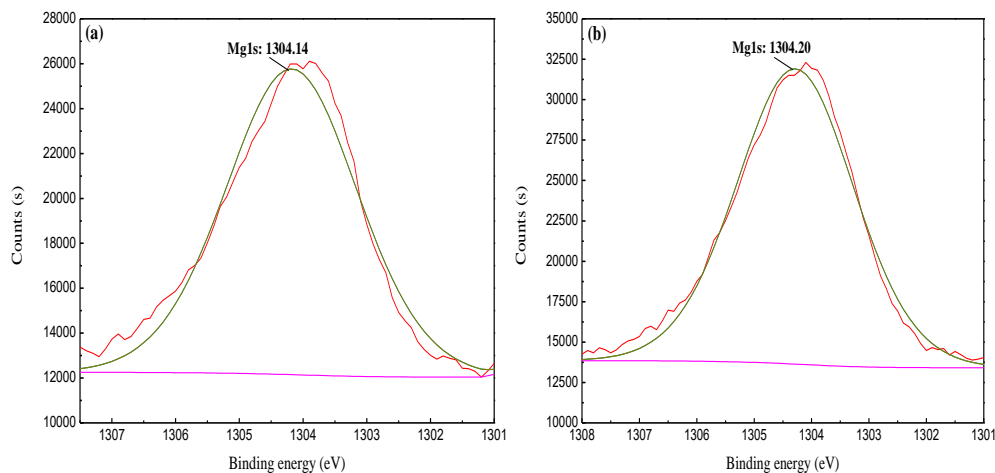
Fig. 11. Plots showing the binding energy of magnesium on magnesite (a) before and (b) after treatment with MSP
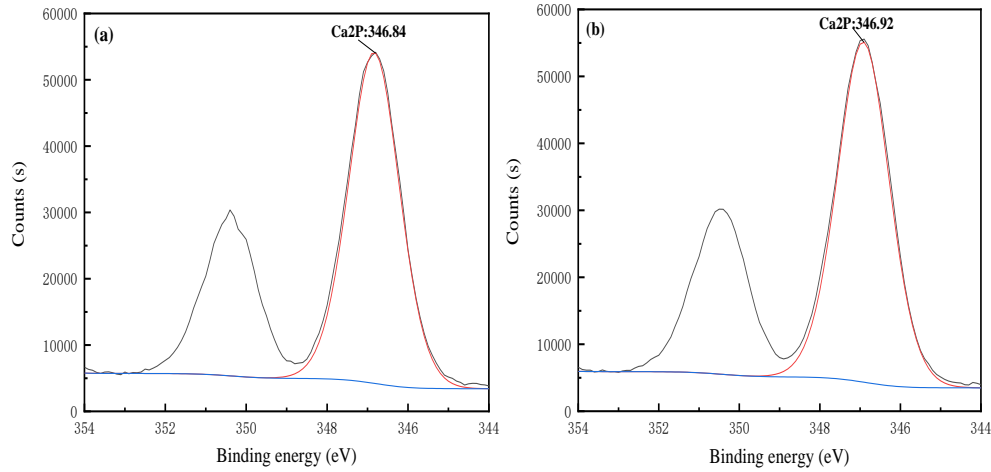
Fig. 12. Plots showing the binding energy of calcium on calcite (a) before and (b) after treatment with MSP

3.5. Chemical composition analysis of the solution

The dissolved components of minerals and reagents in aqueous solutions are closely related to the floatability of minerals. Therefore, this section first investigates the dissolution balance of magnesite and calcite, then investigates the dominant component of DDA in the test, and finally studies the main component of MSP that plays a vital role in the test. The relationship between dissolved components and pH is drawn, providing a theoretical basis for the flotation separation of magnesite and calcite.

3.5.1. Solution chemistry of collector

Lauryl amine of molecular formula $C_{12}H_{25}NH_2$ has a molecular weight of 185.35. DDA is a primary amine in terms of the substituted light numbers and may be abbreviated as RNH_2. Due to the low solubility of DDA in aqueous solutions, the collector was dissolved in aqueous hydrochloric acid and used after generating hydrochloride in the test. In water, the equilibrium of DDA is as follows:

$$RNH_2(s) \rightleftharpoons RNH_2(aq) \qquad\qquad S = 10^{-4.69} = 2.0 \times 10^{-5}\ mol/L \qquad (3.1)$$

$$RNH_2 + HCl \rightleftharpoons RNH_2 \cdot HCl \qquad\qquad\qquad\qquad (3.2)$$

$$RNH_2 \cdot HCl \rightleftharpoons RNH_3^+ + Cl^- \qquad\qquad\qquad\qquad (3.3)$$

$$RNH_3^+ \rightleftharpoons RNH_2(aq) + H^+ \qquad\qquad K_a = 10^{-10.63} = 2.3 \times 10^{-11} \qquad (3.4)$$

$$RNH_2(aq) + H_2O \rightleftharpoons RNH_3^+ + OH^- \qquad K_b = 10^{-3.37} = 4.3 \times 10^{-4} \qquad (3.5)$$

$$2RNH_3^+ \rightleftharpoons (RNH_3^+)_2^{2+} \qquad\qquad K_d = 10^{2.08} = 0.0083 \qquad (3.6)$$

$$RNH_3^+ + RNH_2(aq) \rightleftharpoons RNH_3^+ \cdot RNH_2(aq) \qquad K_{im} = 10^{3.12} = 1.32 \times 10^3 \qquad (3.7)$$

According to Equations (3.1)–(3.7), the concentration logarithm of each component of DDA was calculated when the DDA concentration was $C_T = 1.62 \times 10^{-4}$, as shown in Fig. 13.

The critical pH of DDA is 9.82. In a strongly alkaline solution with pH > 9.82, DDA mainly exists as amine molecules or molecular ion copolymers. When the solution's pH is below the critical pH value, DDA exists mainly as ions. The interaction between DDA and the mineral surface is primarily caused by the cation RNH_3^+ or $RNH_2 \cdot RNH_3^+$ on the mineral surface of the double electric layer. It relies on the electrostatic attraction of adsorption on the mineral surface's negative charge so that the mineral hydrophobic floats.

3.5.2. Solution chemistry of the regulator

MSP of molecular formula NaH_2PO_4 has a molecular weight of 119.96, which is an inorganic acid salt. It is hydrolyzed in water by pressing the following equations:

$$NaH_2PO_4 + H_2O \rightleftharpoons H_3PO_4 + NaOH \qquad\qquad\qquad (3.8)$$

$$PO_4^{3-} + H^+ \rightleftharpoons HPO_4^{2-} \qquad\qquad K_1^H = 10^{12.35} \qquad (3.9)$$

$$HPO_4^{2-} + H^+ \rightleftharpoons H_2PO_4^- \qquad\qquad\qquad K_2^H = 10^{7.2} \qquad\qquad (3.10)$$

$$H_2PO_4^- + H^+ \rightleftharpoons H_3PO_4 \qquad\qquad\qquad K_3^H = 10^{2.15} \qquad\qquad (3.11)$$
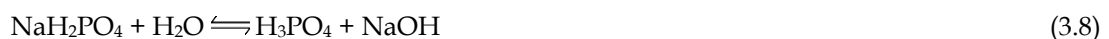
$$\beta_2^H = K_1^H \cdot K_2^H = 10^{19.55} \qquad\qquad\qquad\qquad\qquad\qquad (3.12)$$

$$\beta_3^H = K_1^H \cdot K_2^H \cdot K_3^H = 10^{21.7} \qquad\qquad\qquad\qquad\qquad (3.13)$$

$$C_T = [PO_4^{3-}] + [HPO_4^{2-}] + [H_2PO_4^-] + [H_3PO_4]$$

$$[PO_4^{3-}] = \Phi_0 C_T = C_T / (1 + K_1^H[H^+] + \beta_2^H[H^+]^2 + \beta_3^H[H^+]^3)$$

$$[HPO_4^{2-}] = \Phi_1 C_T = K_1^H \Phi_0 [H^+] C_T$$

$$[H_2PO_4^-] = \Phi_2 C_T = \beta_2^H \Phi_0 [H^+]^2 C_T \qquad\qquad\qquad\qquad (3.14)$$

$$[H_3PO_4] = \Phi_3 C_T = \beta_3^H \Phi_0 [H^+]^3 C_T$$

Equation (3.14) can be derived from Equations (3.8)–(3.13), and the logC-pH relationship diagram of hydrolyzed components of NaH_2PO_4 can be obtained from Equation (3.14), as shown in Fig. 14.
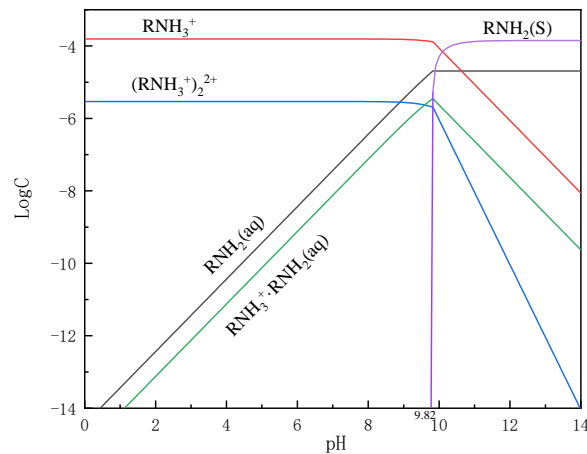
Fig. 13. logC-pH graph of lauryl amine
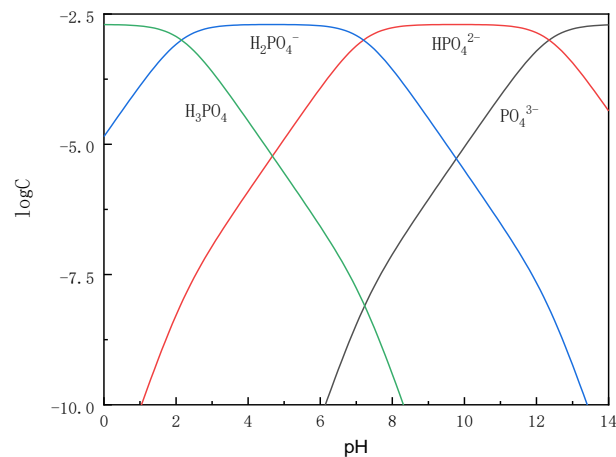
Fig. 14. logC-pH graph of 2×10^{-3} mol/L MSP

The Fig. 14 shows that when pH < 2.2, 2.2 ≤ pH < 7.2, 7.2 ≤ pH < 12.4, and pH ≥ 12.4, the dominant components are H_3PO_4, $H_2PO_4^-$, HPO_4^{2-}, and PO_4^{3-}, respectively. Therefore, in the flotation system of this test, HPO_4^{2-} is the main component that plays a regulating role.

3.5.3. Analysis of adsorption mechanism

The different crystal structures of magnesite and calcite lead to the differences in the exposed ions on their surfaces. In fact, the exposed ions of magnesite and calcite are Ca^{2+} and Mg^{2+}, respectively. When they encounter phosphate root, calcium phosphate and magnesium phosphate precipitate will be

formed. Since the K_{sp} of calcium phosphate (2.07×10^{-33}) is smaller than that of magnesium phosphate (1.04×10^{-24}), it can be inferred that calcium phosphate is more easily formed in solution and thus adsorbed on mineral surfaces (Linke, 1958).
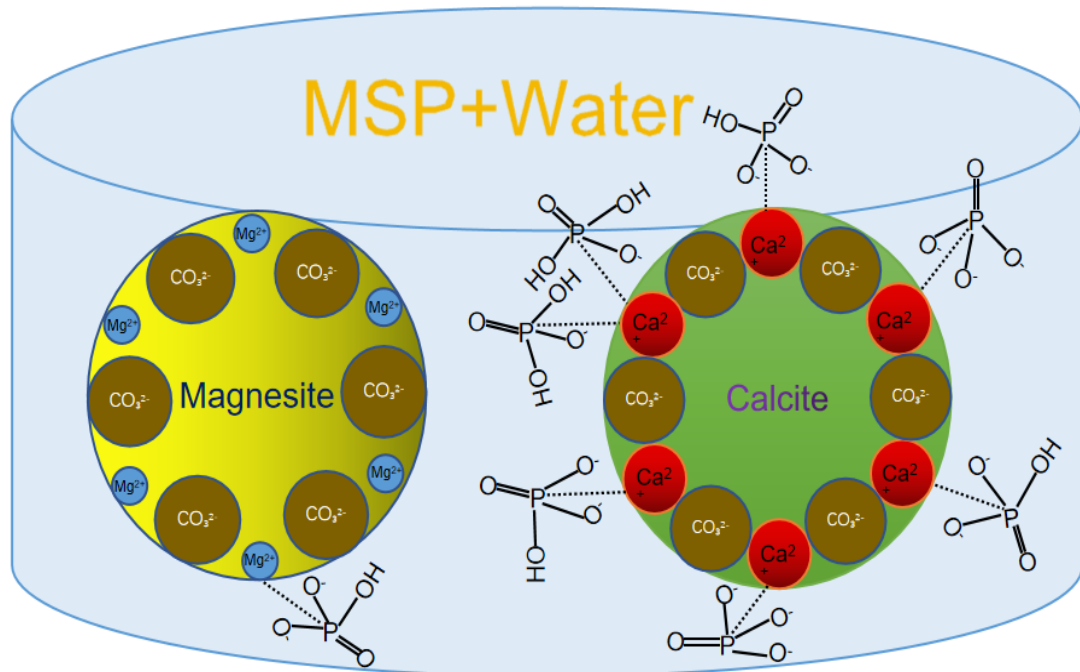
Fig. 15. Adsorption of MSP in water

Fig. 15 shows the mechanism of MSP selectively binding to Ca^{2+}. In the test, the mineral is dissolved, the pH value is adjusted, and a regulator is added to stir evenly. At this time, the regulator interacts with the mineral surface. According to Fig. 14, under alkaline conditions, there are phosphoric groups in MSP, mainly in the form of HPO_4^{2-}, PO_4^{3-} and $H_2PO_4^{-}$, and selectively combine with Ca^{2+}. Exposure to $-O^{-}$ resulted in a decrease in Ca^{2+} surface potential at the active site, which was consistent with zeta potential measurements of MSP interaction with minerals.
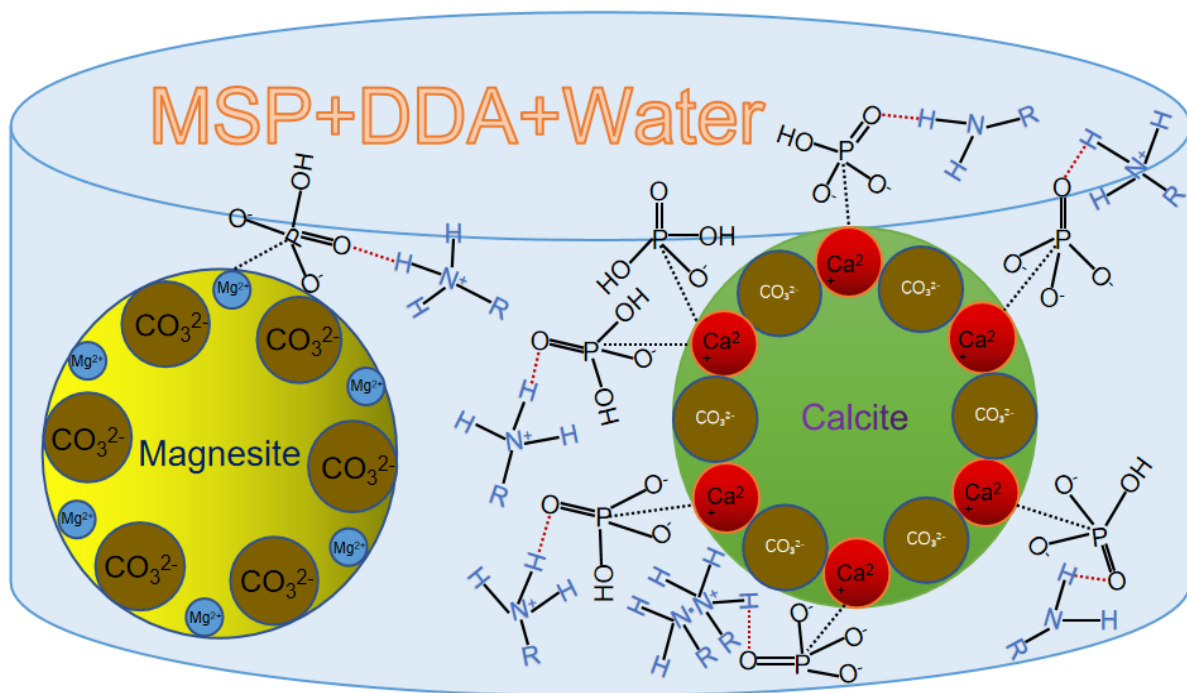
Fig. 16. Adsorption of MSP in water under dodecylamine system

Fig. 16 reflects the separation mechanism of magnesite and calcite. The adsorption differences of MSP on the calcite and magnesite surface lead to different adsorption behaviors of DDA on Ca^{2+} and Mg^{2+}. When considering the alkaline conditions presented in Fig. 13, DDA mainly exists in the forms of RNH_3^+, $RNH_2(aq)$, and $RNH2 \cdot RNH_3^+$. In case of calcite, HPO_4^{2-} and $H_2PO_4^-$ adsorbed onto the Ca^{2+} surface and bonded with $RNH_2(aq)$, RNH_3^+, and $RNH_2 \cdot RNH_3^+$ via hydrogen bonds. Simultaneously, PO_4^{3-} combined with Ca^{2+} to generate negative $CaPO_4^-$, $CaPO_4^-$ combined with RNH_3^+ and $RNH_2 \cdot RNH_3^+$ through electrostatic attraction, increasing the potential of the calcite surface, which was consistent with the measurement results of zeta potential between MSP and mineral in the DDA system. In case of magnesite, MSP is basically not adsorbed on its surface, which is consistent with the change of its zeta potential. Compared with Mg^{2+}, Ca^{2+} has a larger ionic volume (ion radius), resulting in MSP having a better affinity for Ca^{2+}. XPS analysis results show that the relative concentration of elements adsorbed by MSP on the calcite surface is much higher than that of magnesite. Therefore, the exposed Ca^{2+} on mineral surfaces contributes to the adsorption of MSP compared to Mg^{2+}.

4. Conclusions

In this study, the effective components of the flotation agent for the flotation activity of minerals and the optimum conditions for the interaction between the flotation agent and minerals were discovered and verified using detection methods based on the flotation solution chemistry and the dissolution characteristics of minerals, dissolution, dissociation, and association balance of flotation agent in the solution. The effects of collector dosage, regulator dosage, and pulp pH on the floatability of magnesite and calcite in the DDA system were systematically studied, and the best reagent system for flotation separation of magnesite and calcite was determined. The main results are summarized below.

(1) In the DDA flotation system, magnesite and calcite were effectively separated when the pulp pH was 10 and the DDA and MSP dosages were 30 and 240 mg/L, respectively.

(2) The zeta potential measurement showed that MSP-containing negative groups can selectively reduce the zeta potential of calcite and promote the adsorption of DDA-containing positive groups on the surface of the calcite. However, it had little effect on the zeta potential of magnesite.

(3) FTIR and XPS measurements revealed that MSP was adsorbed onto the calcite surface mainly via hydrogen bonds and selectively reacted with calcium; however, this reaction did not occur on the magnesite surface.

References

BOTERO, A.E.C., TOREM, M.L. DE MESQUITA, L.M.S., 2008. *Surface chemistry fundamentals of biosorption of Rhodococcus opacus and its effect in calcite and magnesite flotation*, Minerals Engineering, 21, 83-92.

Brik, M.G. 2011. *First-principles calculations of structural, electronic, optical and elastic properties of magnesite $MgCO_3$ and calcite $CaCO_3$*, Physica B-Condensed Matter, 406, 1004-12.

BOTERO, A.E.C., TOREM, M.L. DE MESQUITA, L.M.S., 2007. *Fundamental studies of Rhodococcus opacus as a biocollector of calcite and magnesite*, Minerals Engineering, 20, 1026-32.

CASES, J.M., VILLIERAS, F., MICHOT L.J., BERSILLON J.L., 2002. *Long chain ionic surfactants: the understanding of adsorption mechanisms from the resolution of adsorption isotherms*, Colloids and Surfaces a-Physicochemical and Engineering Aspects, 205, 85-99.

CHEN, G.L., TAO. G., 2004. *Reverse flotation of magnesite by dodecyl phosphate from dolomite in the presence of sodium silicate*, Separation Science and Technology, 39, 377-90.

DENG, R., YANG, X., HU, Y., KU, J., ZUO, W., MA, Y., 2018. *Effect of Fe(II) as assistant depressant on flotation separation of scheelite from calcite,* Minerals Engineering, 118, 133-40.

GAO, Z., SUN, W., HU, Y., 2015. *New insights into the dodecylamine adsorption on scheelite and calcite: An adsorption model*, Minerals Engineering, 79, 54-61.

GUO, J.-X., SHU, S., LIU, X.-L., WANG, X.-J., YIN, H.-Q., CHU, Y.-H., 2017. *Influence of Fe loadings on desulfurization performance of activated carbon treated by nitric acid*, Environmental Technology, 38, 266-76.

HOU, Q., LUO, X., LI, M., AN, D., XIE, Z., 2021. *Non-isothermal kinetic study of high-grade magnesite thermal decomposition and morphological evolution of MgO*, International Journal of Applied Ceramic Technology, 18, 765-72.

LI, P., DAI, S., SUN, W., FAN, M., 2021. *Study on regulators of purifying magnesite ore by cationic reverse flotation,* Scientific Reports, 11.

LINKE, W.F., SEIDELL, A. 1958. *Solubilities-Inorganic and metal-organic compounds', a compilation of solubility data from the periodical literature*, II.

LU, Y.-P., ZHANG, M.-Q., FENG, Q.-M., LONG, T., OU, L.-M., ZHANG. G.-F., 2011. *Effect of sodium hexametaphosphate on separation of serpentine from pyrite*, Transactions of Nonferrous Metals Society of China, 21, 208-13.

LUO, N., WEI, D., SHEN, Y.,BHAN, C., ZHANG, C,. 2017. *Elimination of the Adverse Effect of Calcium Ion on the Flotation Separation of Magnesite from Dolomite*, Minerals, 7.

MATIS, K.A., BALABANIDIS, T.N., GALLIOS, G.P., 1988. *Processing of magnesium carbonate fines by dissolved-air flotation*, Colloids and Surfaces, 29: 191-203.

MOMENZADEH, L., MOGHTADERI, B., LIU, X.F., SLOAN, S.W., BELOVA, I.V., MURCH, G.E., *The thermal conductivity of magnesite, dolomite and calcite as determined by molecular dynamics simulation*, In, 18-34. Trans Tech Publ.

SANCHEZ-ESPANA, J., DE CORTAZAR, A.G., GIL, P., VELASCO, F., 2002. *The discovery of the Borobia world-class stratiform magnesite deposit (Soria, Spain): a preliminary report*, Mineralium Deposita, 37, 240-43.

SHUAI, S., LIU, Y., ZHAO, C., ZHU, H., LI, Y., ZHOU, K., GE, W., HAO, J., 2020. 'Improved synthesis of graphene oxide with controlled oxidation degree by using different dihydrogen phosphate as intercalators', Chemical Physics, 539.

SONG, S., LOPEZ-VALDIVIESO, A., MARTINEZ-MARTINEZ, C., TORRES-ARMENTA, R., 2006. *Improving fluorite flotation from ores by dispersion processing*, Minerals Engineering, 19, 912-17.

SUN, H., HAN, F., YIN, W.-Z., HONG, J., YANG, B., 2020. *Modification of selectivity in the flotation separation of magnesite from dolomite*, Colloids and Surfaces a-Physicochemical and Engineering Aspects, 606.

SUN, H., YANG, B., ZHU, Z., YIN, W., SHENG, Q., HOU, Y., YAO, J., 2021. *New insights into selective-depression mechanism of novel depressant EDTMPS on magnesite and quartz surfaces: Adsorption mechanism, DFT calculations, and adsorption mode*l. Minerals Engineering 160.

SUN, W., DAI, S., LIU, W., LI, P., DUAN, H., YU, X., 2021. *Effect of Ca(II) on anionic/cationic flotation of magnesite ore*, Minerals Engineering, 163.

SUN, W, LIU, W., DAI, S., YANG, T., DUAN, H., LIU, W., 2020. *Effect of Tween 80 on flotation separation of magnesite and dolomite using NaOL as the collector*, Journal of Molecular Liquids, 315.

TANG, Y., KELEBEK, S., YIN, W., 2020. *Surface chemistry of magnesite and calcite flotation and molecular dynamics simulation of their cetyl phosphate adsorption*, Colloids and Surfaces a-Physicochemical and Engineering Aspects, 603.

TANG, Y., YIN, W., KELEBEK, S., 2020. *Selective flotation of magnesite from calcite using potassium cetyl phosphate as a collector in the presence of sodium silicate*, Minerals Engineering, 146.

TENG, Q., FENG, Y., LI, H., 2018. *Effects of silicate-bacteria pretreatment on desiliconization of magnesite by reverse flotation,* Colloids and Surfaces a-Physicochemical and Engineering Aspects, 544, 60-67.

WANG, J., GAO, Z., GAO, Y., HU, Y., SUN, W., 2016. *Flotation separation of scheelite from calcite using mixed cationic/anionic collectors*, Minerals Engineering, 98, 261-63.

WEI, J., GE, J., ROUFF, A.A., WEN, X., MENG, X., SONG, Y., 2019. *Phosphorus recovery from wastewater using light calcined magnesite, effects of alkalinity and organic acids*, Journal of Environmental Chemical Engineering, 7.

WONYEN, D.G., KROMAH, V., GIBSON, B., NAH, S., CHELGANI, S.C., 2018. *A Review of Flotation Separation of Mg Carbonates (Dolomite and Magnesite)*, Minerals, 8.

YANG, B., SUN, H., WANG, H., YIN, W., CAO, S., WANG, Y., ZHU, Z., JIANG, K., YAO, J., 2020. *Selective adsorption of a new depressant Na(2)ATP on dolomite: Implications for effective separation of magnesite from dolomite via froth flotation*, Separation and Purification Technology, 250.

YANG, B.,, YIN, W., YAO, Y., SHENG Q., ZHU, Z., 2022. *Role of decaethoxylated stearylamine in the selective flotation of hornblende and siderite: An experimental and molecular dynamics simulation study*, Applied Surface Science, 571.

YANMIS, D., ORHAN, F., GULLUCE, M., SAHIN, F., 2015. *Biotechnological magnesite enrichment using a carbonate dissolving microorganism, Lactococcus sp*, International Journal of Mineral Processing, 144, 21-25.

YAO, J., YIN, W., GONG, E., 2016. *Depressing effect of fine hydrophilic particles on magnesite reverse flotation*, International Journal of Mineral Processing, 149: 84-93.

YAO, J., SUN, H., BAN, X., YIN. W., 2021. *Analysis of selective modification of sodium dihydrogen phosphate on surfaces of magnesite and dolomite: Reverse flotation separation, adsorption mechanism, and density functional theory calculations*, Colloids and Surfaces a-Physicochemical and Engineering Aspects, 618.

YAO, J., SUN, H., HAN, F., YIN, W., HONG, J., WANG, J., WON, C., DU, L., 2020. *Enhancing selectivity of modifier on magnesite and dolomite surfaces by pH control*, Powder Technology, 362, 698-706.

YAO, J., SUN, H., YANG, B., ZHOU, Y., YIN, W., ZHU, Z., 2020. *Selective co-adsorption of a novelmixed collector ontomagnesite surface to improve the flotation separation of magnesite from dolomite*, Powder Technology, 371, 180-89.

YIN, W., SUN, H., HONG, J., CAO, S., YANG, B., WON, C., SONG, M., 2019. *Effect of Ca selective chelator BAPTA as depressant on flotation separation of magnesite from dolomite*, Minerals Engineering, 144.

YIN, W., YANG, B., FU, Y., CHU, F., YAO, J., CAO, S., ZHU, Z., 2019. Effect of calcium hypochlorite on flotation separation of covellite and pyrite, Powder Technology, 343: 578-85.

YUAN, S., WANG, R., GAO, P., HAN, Y., LI, Y., 2022. *Suspension magnetization roasting on waste ferromanganese ore: A semi-industrial test for efficient recycling of value minerals*, Powder Technology, 396: 80-91.

ZHAO, Z., CUT, X., WANG, D., CHEN, Y., BAI, G., LI, J., LIU, X., . 2015. *Review of the Metallogenic Regularity of Magnesite Deposits in Chin*a, Acta Geologica Sinica-English Edition, 89, 1747-61.